Low-frequency elastic properties of the incommensurate ferroelastic $[N(CH_3)_4]_2CuCl_4$

A. V. Kityk,* V. P. Soprunyuk,* A. Fuith, W. Schranz, and H. Warhanek
Institut fur Experimentalphysik, Universitat Wien, Strudlhofgasse 4, A-1090 Wien, Austria
(Received 12 April 1995; revised manuscript received 21 September 1995)

The low-frequency elastic properties of incommensurate ferroelastic crystals $[N(CH_3)_4]_2CuCl_4$ are studied in the vicinity of the incommensurate phase transitions using parallel-plate-stress and three-point-bending methods. The temperature dependences of the effective elastic constants (relative Young's modulus) along all principal crystal directions and the shear elastic compliance $S_{55}=1/C_{55}$ were obtained. Similarly to the elastic properties at ultrasonic frequencies (10 MHz), the elastic anomalies at low frequencies (5 Hz) near the paraelastic-incommensurate transition (at T_i) are well explained in the framework of the plane-wave approximation. In the transition region from the incommensurate to the commensurate improper ferroelastic phase we apply soliton theory. From the experimental data it follows that the anomalous behavior of S_{55} near the phase transition from incommensurate to commensurate improper ferroelastic phase has the same features as the dielectric constant in the vicinity of incommensurate-commensurate improper ferroelectric phase transition, including the Curie-Weiss-type anomaly for $S_{55}(T)$ near T_c, thermal hysteresis phenomena, and similar changes in the character of the anomaly under applied static stress σ_5. The last results are explained within the framework of soliton theory proposed by Holakovsky and Dvorak [J. Phys. C **21**, 5449 (1988)].

I. INTRODUCTION

The behavior of dielectric susceptibility χ near the phase transition from the incommensurate (IC) to the commensurate (C) improper ferroelectric phase (at $T=T_c$) is usually described by a Curie-Weiss-type anomaly. The origin of this anomaly is connected with the multisoliton lattice which usually exists in the IC phase. Near T_c as a matter of fact the multisoliton lattice may be represented as a periodic sequence of nearly commensurate regions (quasidomains) with an opposite orientation of polarization $^{\pm}P_0$ separated by discommensurations (domain walls) where the phase of the IC modulation wave changes rapidly.[1,2] Under an applied electric field the walls shift along the modulation axis, extending the region of the preferred polarization at the expense of the opposite polarization.[3] The displacements of the walls become remarkable especially in the region of the IC-C phase transitions, i.e., the distance x_0 between walls diverges logarithmically at T_c and the walls interact no longer. In other words the discommensurations can move freely in an oscillating electric field and consequently the dielectric susceptibility χ diverges at T_c. The pinning of phase solitons by defects causes the observed global thermal hysteresis effect which is clearly seen in the vicinity of the IC-C phase transition.[4] According to earlier theories[5,6] the Curie-Weiss-type behavior for dielectric properties should persist in an applied static electric field E_s with the only difference that the anomaly becomes sharper and shifts to higher temperatures. This, however, has not been confirmed experimentally. Even in a zero static field, χ does not diverge but attains only a maximum which then shifts under applied field to higher temperatures and gradually decreases.[7] This result was explained later by Holakovsky and Dvorak.[8] Their theory was based on the assumption that domain walls in an applied static field E_s and measuring components field δE can only oscillate around their equilibrium positions corresponding to E_s without any change of the total period of IC modulation.

The theories mentioned above can be easily transformed into the case of improper incommensurate ferroelastics. In analogy one can expect that the anomalous behavior of some components of the elastic compliance S_{ij} near the IC-C improper ferroelastic phase transition will possess the same features as the dielectric susceptibility χ in the vicinity of the IC-C improper ferroelectric phase transition. This includes a Curie-Weiss-type anomaly for $S_{ij}(T)$ near T_c, thermal hysteresis phenomena, and a similar change in the character of the anomaly under applied static component of stress. In the present paper we report original experimental results of a low-frequency (1–15 Hz) elastic study of the improper incommensurate ferroelastics tetramethylammonium tetrachlorocuprate $[N(CH_3)_4]_2CuCl_4$ (TMATC-Cu) in the region of phase transitions into the IC phase. This crystals belong to the large group of A_2BX_4 compounds with a β-K_2SO_4-type structure in the high-temperature paraelastic (P) phase, space group $Pmcn$ (D_{2h}^{16}). On cooling they undergo successive phase transitions into the IC phase at $T_i=298$ K and to the monoclinic improper ferroelastic C phase [space group $P12_1/c1$ (C_{2h}^5)] at $T_c=292$ K.[9] The static displacement below T_i corresponds to the condensed soft mode at wave vector $k_0=(2\pi/c)(1/3-\delta)$, where $\delta=0.007$ and is independent on temperature. On further cooling, another monoclinic proper ferroelastic phase [space group $P112_1/m$ (C_{2h}^5)] appears below $T_1=263$ K. Ultrasonic studies showed an additional phase transition at $T_2=127$ K but the symmetry of the low-temperature phase is still unknown.[10] Phase transitions in TMATC-Cu crystals have been studied by various experimental techniques: neutron diffraction,[9] Raman scattering, dilatometric, and heat-capacity measurements,[11] dielectric and ultrasonic measurements,[10,12–16] optical birefringence and optical-microscope observations of the domain structure.[11,12,14,15] Particularly, ultrasonic measurements[13] have revealed a remarkable change of the shear elastic constant C_{55} (Fig. 1) in the vicinity of the IC-C phase transition. The elastic constant C_{55} shows a clear change in slope at T_i,

 © 1996 The American Physical Society

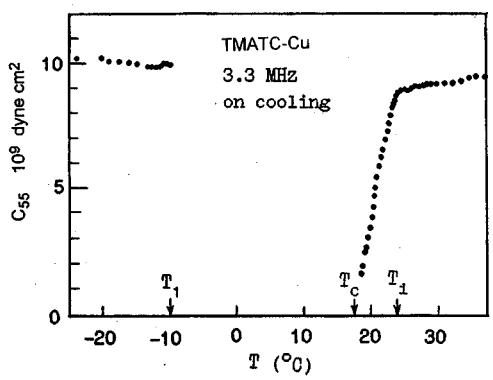

FIG. 1. Variation of the elastic constant C_{55} in the region of the phase transitions of TMATC-Cu crystals (Ref. 13).

then decreases rapidly and tends to vanish towards the IC-C phase transition. Unfortunately these measurements were not performed in the region of the C phase due to the strong attenuation of the ultrasound waves. Thus the total picture of the elastic behavior around the IC-C phase transition has not been ascertained. This problem is solved firstly in the present work. This aim was achieved using low-frequency dynamical mechanical analysis (DMA) methods for the elastic measurements. Simultaneously we present also some results of ultrasonic measurements for comparison with the results of DMA measurements. In contrast to previous considerations[10,13,15] the obtained results are explained within the framework of plane-wave and soliton models.

II. EXPERIMENTAL

The TMATC-Cu crystals were grown by slow evaporation at 300 K from an aqueous solution containing a stoichiometric molar ratio of $N(CH_3)_4Cl$ and $CuCl_2$. The crystallographic axis were determined by the x-ray diffraction: $a=9.039$ Å, $b=15.155$ Å, $c=12.127$ Å in accordance with Ref. 14. Ultrasonic studies have been done by the pulse-echo overlap technique.[17] The longitudinal acoustic waves were excited by a $LiNbO_3$ piezoelectric transducer at the frequency of 10 MHz.

The low-frequency elastic measurements were performed by the parallel-plate-stress (PPS) and three-point-bending (TPB) methods using a dynamical mechanical analyzer DMA-7, Perkin-Elmer. The sample geometries for both methods are presented in Fig. 2. The relations between the effective spring constant k measured by DMA-7 and Young's modulus Y are determined as[18]

$$k=Y(q)4b\left(\frac{h}{L}\right)^3\left[1+\frac{3}{2}\left(\frac{h}{L}\right)^2\frac{Y(q)}{G(pq)}\right]^{-1}, \quad \text{(TPB method)} \tag{1}$$

$$k=Y(q)\frac{S}{h}, \quad \text{(PPS method)} \tag{2}$$

where the geometrical parameters of the sample b, h, L, and S are given in Fig. 2, $Y(q)$ is Young's modulus in the q direction, and $G(pq)$ is the shear modulus. Thus using both methods and combining different measuring geometries, it is possible to determine the desired elastic constant. Since the absolute accuracy of such measurements is usually not better than 20% the corresponding results are presented in a relative form. The relative accuracy in the last case was about 1%. Elastic measurements have been performed at cooling and heating runs with a rate of temperature change of 0.15–0.6 K/min.

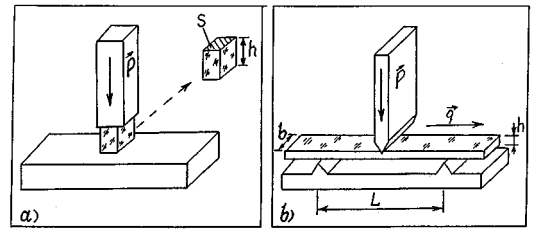

FIG. 2. Typical sample geometries for the PPS (a) and TPB (b) methods. P is the load, b is the specimen width, h is the specimen thickness, L is the span, and S is the base area.

III. EXPERIMENTAL RESULTS AND DISCUSSION

A. Elastic properties at low biasing stress

Unfortunately, the dynamical PPS and TPB methods do not provide the possibility for elastic measurements without a biasing stress σ_s. σ_s is proportional to the applied constant load P_s. For a reason of sample stability in the measuring cell the static component P_s of the total load $P=P_s+\delta P$ (Fig. 2) should not be less than the ac component δP, i.e., the condition $\delta P<P_s$ must be satisfied. However the value of δP may chosen to be small, so that we can easily satisfy the condition of the biasing stress to be almost zero. This point is very important for the further explanation of our results within the framework of the present theories. The influence of the applied biasing stress on the elastic anomalies will be considered in Sec. III C.

The temperature dependences of the real parts of the relative effective elastic constants $C_r'=C'/C_0'$ ($f=5$ Hz) along all principal crystallographic directions for TMATC-Cu crystals, obtained by the PPS method, are presented in Fig. 3. In that case the changes of effective elastic constants C_r' are associated with the temperature behavior of Young's modulus $Y(a)=1/S_{11}$, $Y(b)=1/S_{22}$, and $Y(c)=1/S_{33}$, respectively, ($C_r'=Y/Y_0$), where the elastic compliancies S_{ii} can be expressed through the elastic constant as follows:

$$1/S_{11}=C_{11}+\frac{2C_{12}C_{23}C_{13}-C_{13}^2C_{22}-C_{12}^2C_{33}}{C_{22}C_{33}-C_{23}^2},$$

$$1/S_{22}=C_{22}+\frac{2C_{12}C_{23}C_{13}-C_{12}^2C_{33}-C_{23}^2C_{11}}{C_{11}C_{33}-C_{13}^2}, \tag{3}$$

$$1/S_{33}=C_{33}+\frac{2C_{12}C_{23}C_{13}-C_{13}^2C_{22}-C_{23}^2C_{11}}{C_{11}C_{22}-C_{12}^2}.$$

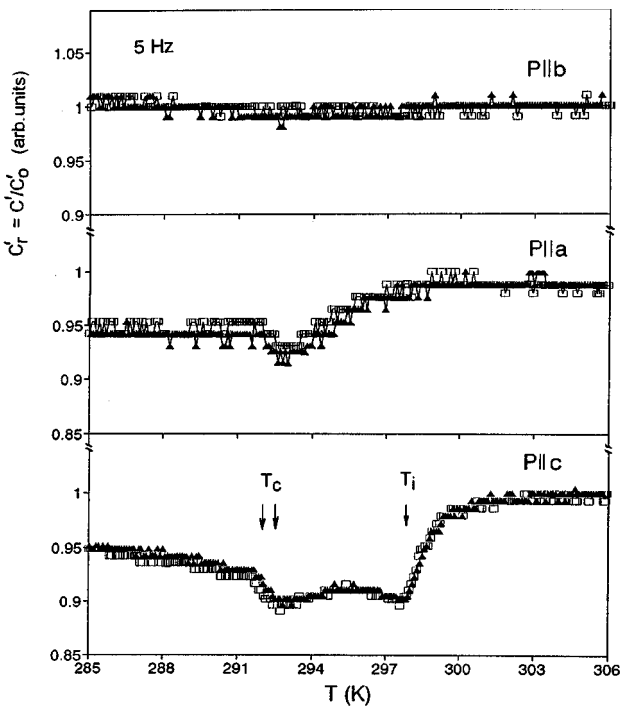

FIG. 3. Temperature dependence of the real part of effective elastic constants C'_r measured by the PPS method. The load $P=P_s+\delta P$ is parallel to the principal crystallographic directions. C'_0 corresponds to $T=302$ K. □ indicates cooling; ▲ indicates heating.

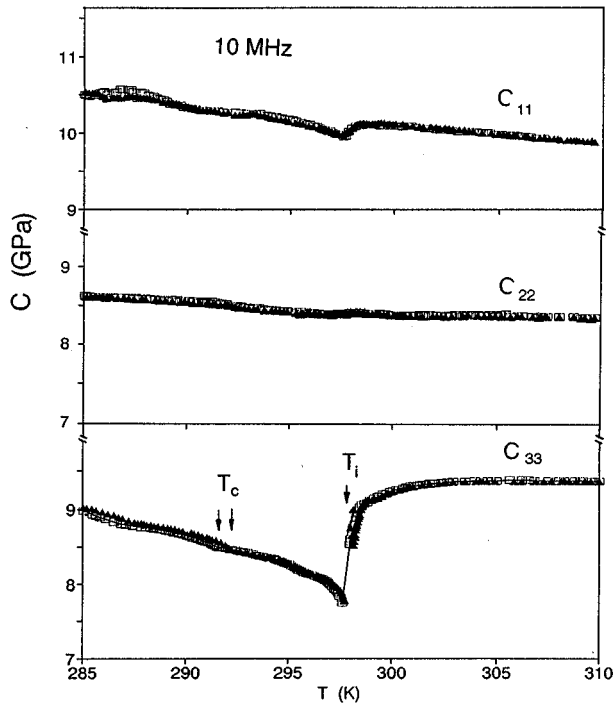

FIG. 4. Temperature dependence of the longitudinal elastic constants $C_{ii}(i=1-3)$ (ultrasonic measurements). □ indicates cooling; ▲ indicates heating.

For comparison, the dependences $C'_{11}(T)$, $C'_{22}(T)$, and $C'_{33}(T)$, obtained from ultrasonic measurements ($f=10$ MHz), are presented in Fig. 4. Both methods show practically, the same results in the vicinity of the P-IC phase transitions at T_i. The most appreciable softening occurs here in the elastic constant C'_{33} which is in good agreement with previous acoustical measurements.[10,14] From the presented data it follows that the main contributions to the changes of the effective elastic constants $C'_r(i)$ at $T=T_i$ are caused preferably by the first terms of Eq. (3). The anomalous changes of elastic constants C'_{11} and C'_{33} near the IC-C phase transitions are clearly observed only for a frequency of 5 Hz (Fig. 3). In contrast to ultrasonic measurements[16] we have not revealed any anomalies in the imaginary parts for all elastic constants at 5 Hz in the transition regions into the IC phase.

The anomalous behavior of the elastic constants $C'_r(a)$, $C'_r(b)$, and $C'_r(c)$ near the P-IC-C phase transition can be explained within the phenomenological theory by including terms in the free energy which represent the interaction of the deformation component U_i with the order parameter. As usually it is convenient to use as order parameter the normal phonon coordinate Q_k which in the present case belongs to the irreducible representation Σ_2 of the space-group symmetry of the high-temperature P phase. According to Rehwald and Vonlanthen[10] the coupling part of the free-energy density may be presented in the following form:

$$F=\sum_{i=1}^{3} a_i U_i Q_{k_0} Q^*_{k_0}+\frac{1}{2}\sum_{i=1}^{6} b_{ii} U_i^2 Q_{k_0} Q^*_{k_0} + \sum_{\substack{i,j=1\\ i\neq j}}^{3} b_{ij} U_i U_j Q_{k_0} Q^*_{k_0}+\frac{1}{3} f_5 U_5 (Q^{*2}_{k_0} Q_{c*-2k_0}+\text{c.c.}), \tag{4}$$

where Q_{c*-2k_0} is the fluctuation component of the second harmonic of the modulation, created by the deformation component U_5. Generally speaking, the coupling part of free energy (4) corresponds to the case of the plane-wave approximation. Using the normal coordinates of the soft mode (amplitudon and phason)[19] it is possible to express the changes of the real $\Delta C'_{ii}$ and the imaginary $\Delta C''_{ii}$ parts of complex elastic constants in the IC phase like[20,21]

$$\Delta C'_{ii}=b_{ii}Q_0^2-2a_i^2Q_0^2/\omega_A^2(k_0)[1+\Omega^2\tau_A^2(k_0)], \quad i=1-3, \tag{5}$$

$$\Delta C''_{ii}=2a_i^2Q_0^2\Omega\tau_A(k_0)/\omega_A^2(k_0)[1+\Omega^2\tau_A^2(k_0)], \quad i=1-3, \tag{6}$$

$$\Delta C'_{44}=b_{44}Q_0^2; \quad \Delta C''_{44}=0, \tag{7}$$

$$\Delta C'_{66}=b_{66}Q_0^2; \quad \Delta C''_{66}=0, \tag{8}$$

$$\Delta C'_{ij}=b_{ij}Q_0^2-2a_ia_jQ_0^2/\omega_A^2(k_0)[1+\Omega^2\tau_A^2(k_0)],$$
$$\Delta C''_{ij}=2a_ia_jQ_0^2\Omega\tau_A(k_0)/\omega_A^2(k_0)[1+\Omega^2\tau_A^2(k_0)],$$
$$i,j=1-3 \quad i\neq j \quad (9)$$

$$\Delta C'_{55}=b_{55}Q_0^2-\frac{f_5^2Q_0^4}{2}\left[\frac{1}{\omega_A^2(k)[1+\Omega^2\tau_A^2(k)]}+\frac{1}{\omega_\varphi^2(k)[1+\Omega^2\tau_\varphi^2(k)]}\right], \quad (10)$$

$$\Delta C''_{55}=\frac{f_5^2Q_0^4}{2}\left[\frac{\Omega\tau_A(k)}{\omega_A^2(k)[1+\Omega^2\tau_A^2(k)]}+\frac{\Omega\tau_\varphi(k)}{\omega_\varphi^2(k)[1+\Omega^2\tau_\varphi^2(k)]}\right], \quad (11)$$

where $Q_0^2=A(T_i-T)/B$ is the equilibrium value of the order parameter amplitude, Ω is the frequency of the dynamical stress, $\omega_A^2(q)=2A(T_i-T)+hq^2$ and $\omega_\varphi^2(q)=hq^2$ are the amplitudon and phason frequency, respectively, τ_A and τ_φ are the corresponding relaxation times, $k=2\pi/c-3k_0=2\pi\delta/c$. As it follows from Eq. (5), the C'_{11}, C'_{22}, and C'_{33} elastic constants undergo a steplike decrease at T_i ($\Delta C'_{ii}\sim a_i^2/B$) caused by the amplitudon mode. Comparison with experiment (Figs. 3 and 4) shows that the coupling coefficients a_1 and a_2 are negligibly small. Therefore only C'_{33} and consequently $C'_r(c)$ both reveal a remarkable decrease just below T_i. According to (6) the anomalies in the imaginary part at PPS measurements should be smaller by nearly six orders of magnitude than in the ultrasonic experiments. That probably explains the absence of anomalies in the imaginary parts for all elastic constants at low frequencies.

Let us now consider the results, which have been obtained using the TPB method. For different measuring geometries and temperature runs they are presented in Figs. 5 and 6. The components of Young's modulus $Y(q)$ and shear modulus $G(pq)$, which contribute to the effective spring constants k [see Eq. (1)] for different experimental geometries are presented in the Table I. From the experimental data it follows that near the P-IC phase transition only the effective moduli $C'_r=C'/C'_0$, which contain $Y(c)=S_{33}^{-1}$, show the large changes. At the same time, a remarkable gradual decrease of C'_r near the IC-C phase transition takes place only for the effective modulus which contains the contribution of the shear modulus $G(pq)=C_{55}=1/S_{55}$. In the latter case the essential decrease in the real part is accompanied by a clear increase of the imaginary part $C''_r=C'_r tg\,\delta$ near T_c. The change of temperature run is accompanied by the global hysteresis effect around the IC-C phase transition (see Fig. 6). It should be noted that thermal hysteresis do not depend on temperature variation rate in the range 0.15–0.6 K/min. The values of the elastic anomalies for the real and imaginary parts of the effective elastic constant at T_c do not depend on frequency (Fig. 7) in the range of 5–15 Hz.

Summing up the obtained results we can conclude already that a clear anomalous softening of the elastic constants $C'_r(P\|a,q\|c)$, $C'_r(P\|c,q\|a)$, and $C'_r(P\|[210],q\|c)$ as well

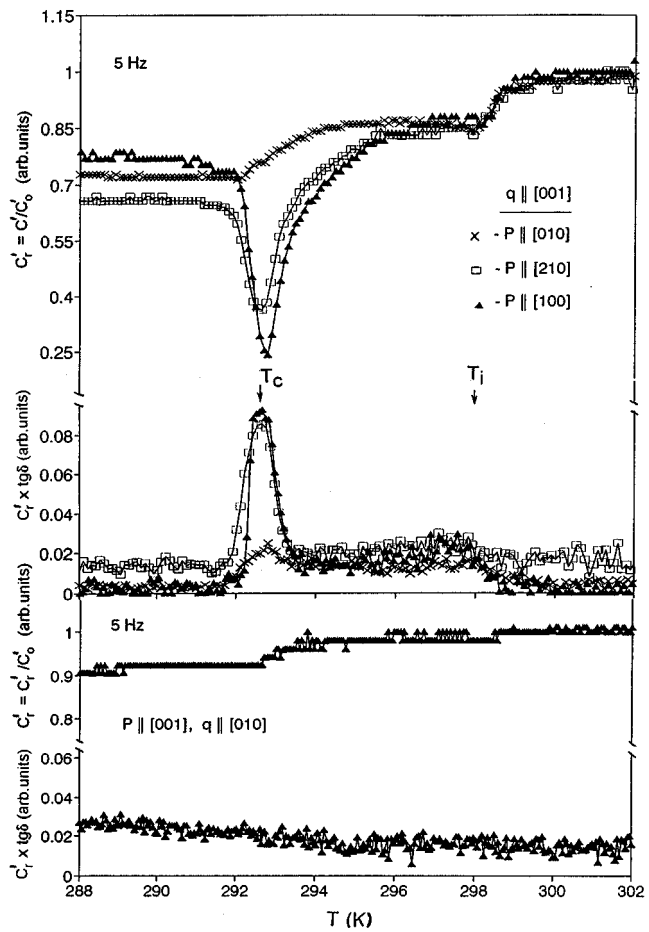

FIG. 5. Measured temperature dependences of the real part C'_r and imaginary part $C'_r tg\,\delta$ of the complex effective elastic constant (on heating) for different sample geometries in the TPB method. C'_0 corresponds to $T=302$ K.

as an increase of the corresponding imaginary parts near T_c is caused by a direct contribution of the complex elastic constant $C^*_{55}=C'_{55}+iC''_{55}$. However, the anomalous behavior of the complex elastic constant C^*_{55} in the vicinity of T_c cannot be explained only by Eqs. (10) and (11). Concerning the real part of C^*_{55}, such clear softening of C'_{55} near T_c does not follow from Eq. (10). Note that the phason frequency $\omega_\varphi^2(k)=h(c^*\delta)^2$ (δ=0.007) according to neutron-scattering measurements,[9] should be constant in the whole temperature range of the IC phase. Since $\tau_\varphi(k)$ and $\tau_A(k)$ are usually of the order of 10^{-9}–10^{-13} s,[22,23] any anomalous changes near T_c at low frequencies Ω should not be observed in the imaginary part C''_{55}. Even in case of unusual large relaxation time Eq. (11) predicts a strong variation of $\Delta C''_{55}$ with frequency in contradiction to the experimental results (see Fig. 7). A possible explanation for the appearance of this frequency-independent loss anomaly would be the presence of a broad distribution of relaxation times with very low-frequency contributions. In this case the operating frequency range (5–15 Hz) would be much too small to probe such a dispersion. To be more specific the unusual temperature behavior of C''_{55} in

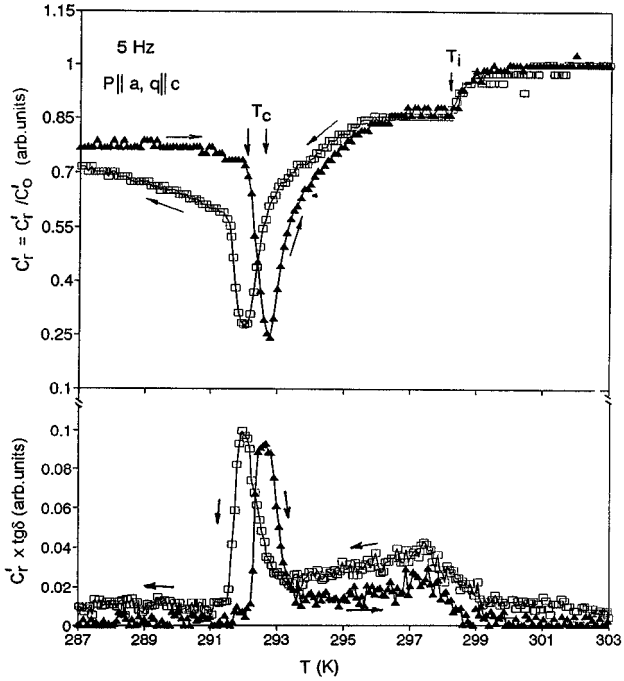

FIG. 6. Measured temperature dependences of the relative real part C_r' and imaginary part $C_r' tg\delta$ of the complex effective elastic constant $C_r^*(P\|a,q\|c)$ in the TPB method at heating (▲) and cooling (□) runs. C_0' corresponds to $T=302$ K.

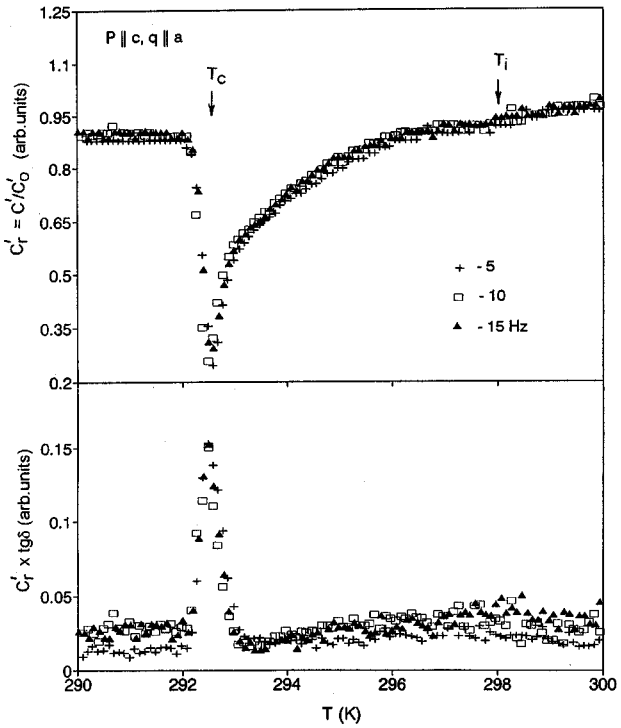

FIG. 7. Measured temperature dependences of the relative real part C_r' and imaginary part $C_r' tg\delta$ of the complex effective elastic constant $C_r^*(P\|c,q\|a)$ (on heating) measured for different frequencies in the TPB method. C_0' corresponds to $T=302$ K.

the region of T_c may be explained at least in two ways. The first one is based on the soliton model; defects and impurities hamper the free motion of soliton under oscillating measuring stress δP and as a result the corresponding oscillating process is accompanied by losses. The second one follows from the coexistence of IC and C structure near T_c;[24] the energy losses appear on the inhomogeneous structure between coexisting phase regions. Both models need further special theoretical considerations. It should be noted that existing soliton theories for IC ferroelectric crystals concern only the anomalous behavior in the real part of the dielectric susceptibility. We will apply one of those theories[8] for the explanation of anomalies in the real part of elastic constants near the IC-C ferroelastic phase transition.

B. Anomalous behavior of the elastic compliance S_{55} near T_c

Using Eq. (1), the elastic compliance $S_{55}=1/C_{55}$ can be easily obtained from the experimental data, presented in Figs. 3, 6, and 7. The temperature dependences of the relative elastic compliance $S_{55}^r=S_{55}/S_{55}^0$, recalculated in that way, are presented in Fig. 8 for cooling and heating runs. As usual, the S_{55}^0 value corresponds to $T=302$ K. It follows from Fig. 8 that the temperature behavior of S_{55}^r near T_c displays the same peculiarities as the temperature dependence of the dielectric constant in the region of the IC improper ferroelectric phase transition. That is:

TABLE I. The components of Young's modulus $Y(q)$ and shear modulus $G(pq)$ for different geometry of measurements in the TPB method [see Eq. (1)].

Sample geometry	$Y(q)$	$G(pq)$
$P\|[010]$, $q\|[001]$	S_{33}^{-1}	S_{44}^{-1}
$P\|[210]$, $q\|[001]$	S_{33}^{-1}	$(S_{44}/5+4S_{55}/5)^{-1}$
$P\|[100]$, $q\|[001]$	S_{33}^{-1}	S_{55}^{-1}
$P\|[001]$, $q\|[010]$	S_{22}^{-1}	S_{44}^{-1}
$P\|[001]$, $q\|[100]$	S_{11}^{-1}	S_{55}^{-1}

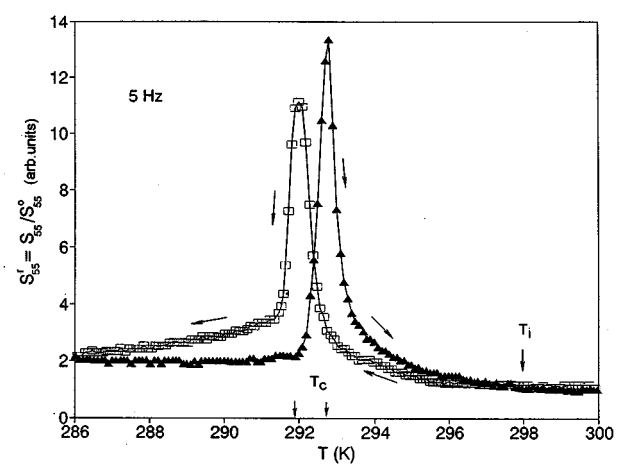

FIG. 8. Temperature dependences of the relative elastic compliance $S_{55}^r=S_{55}/S_{55}^0$ (S_{55}^0 corresponds to $T=302$ K) calculated from the experimental data presented in Figs. 3 and 6. ▲ indicates heating; □ indicates cooling.

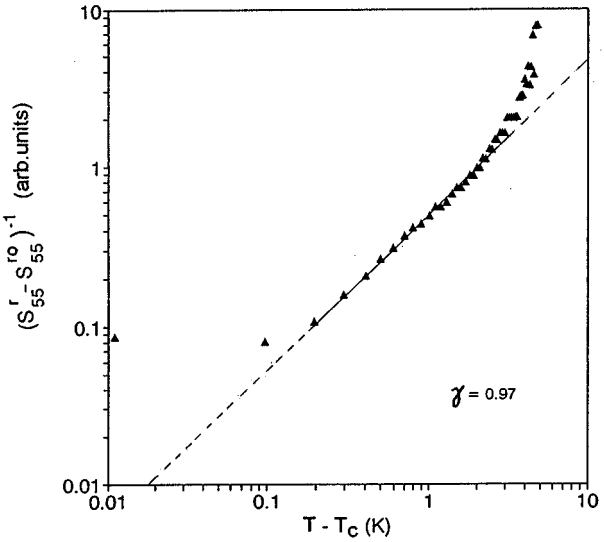

FIG. 9. log-log plot of the reciprocal elastic compliance vs T-T_c in the IC phase of TMATC-Cu crystals ($S^{r0}_{55}=1$).

(i) On heating the dependence of $S^r_{55}(T)$ is sharp below T_c and gradual above T_c, while on cooling the temperature changes S^r_{55} are gradual for both sides around the IC-C ferroelastic phase transition;

(ii) the change of the temperature run is accompanied by a clear thermal hysteresis near T_c;

(iii) the temperature behavior of S^r_{55} in the region $T_c+0.2-T_c+2.5$ K follows a Curie-Weiss law $[S^r_{55}-S^{r0}_{55}\sim(T-T_c)^{-\gamma}]$ with a critical exponent $\gamma=0.97\pm0.02$ (Fig. 9).

Let us consider the last result within the framework of the soliton model, proposed earlier by Holakovsky and Dvorak[8] for the explanation of dielectric anomalies in the vicinity of the phase transitions from IC to the C improper ferroelectric phase. We are reproducing here only the general points of the above theory adding some corrections due to the improper ferroelastic nature of IC-C phase transition. In other words we will consider the anomalous behavior of the elastic compliance S_{55} near the IC-C improper ferroelastic phase transition of TMATC-Cu crystals using the complete analogy between IC ferroelectrics and ferroelastics. Following Ishibashi[25] the spatial modulation of the order parameter Q as well as the shear component of spontaneous deformation U_5 in the IC phase may be written in terms of a Fourier expansion:

$$Q(z)=\sum_{n=0} a_{6n+1}e^{i(6n+1)k_0z}+\sum_{n=1} a_{6n-1}e^{-i(6n-1)k_0z}, \tag{12}$$

$$U_5(z)=\sum_{n=0} d_{6n+3}\sin(6n+3)k_0z, \tag{13}$$

where a_{6n+1}, a_{6n-1}, and d_{6n+3} are the amplitude of the corresponding harmonics. Just below T_i only the main harmonics a_1 and d_3 are important. As the temperature becomes lower, the higher harmonics grow up leading to the appearance of a domainlike (soliton) structure. The latter is schematically presented in Fig. 10. This soliton structure consists of a sequence of almost C regions separated by discommensurations (domain walls). Such a multisoliton state can be defined by the following expression for the difference between the free-energy densities of IC and C phases:[2]

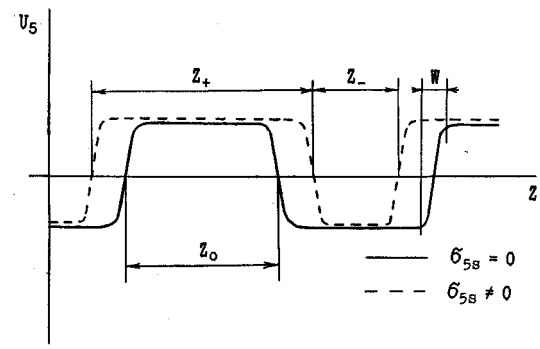

FIG. 10. Schematic representation of the effect of shear stress component σ_5 on the domainlike structure near the IC-C improper ferroelastic phase transition.

$$f=f_{\rm ic}-f_{\rm c}=\frac{1}{z_0}[-bt+4b\ \exp(-z_0/w)], \tag{14}$$

where $t=a(T-T_c)$, $a>0$, z_0 is the distance between walls, and w is the domain-wall width (Fig. 10). This equation is valid only for a well developed domainlike structure, that is the condition $w/z_0\ll1$ should be satisfied. Under applied stress $\sigma_5=\sigma_{5s}+\delta\sigma_5$ (σ_{5s} and $\delta\sigma_5$ are the static and oscillating parts, respectively) the width z_+ of domains with $U_5(+)$ enlarges, while the width z_- with $U_5(-)$ shrinks (Fig. 10). $z_++z_-=2z_0$ corresponds to a new period of IC phase under the applied stress σ_5. Following Holakovsky and Dvorak[8] we assume that z_0 is a function of the static stress σ_{5s} only and does not depend on the oscillating part of the stress $\delta\sigma_5$. This means that we consider a so-called "clamped" compliance at constant $2z_0(\sigma_{5s})$, i.e., $(\partial z_+/\partial\sigma_5)_{z_0}=-(\partial z_-/\partial\sigma_5)_{z_0}$. The deformation of the system due to discommensuration shifts is

$$U_{50}=U_{50}(z_+-z_-)/(z_++z_-)=U_{50}(1-z_-/z_0), \tag{15}$$

where U_{50} is the spontaneous deformation within a single domain. In presence of an external stress σ_5 the energy of the system has the form

$$f(\sigma_5)=(z_++z_-)^{-1}[-2bt+4b\ \exp(-z_+/w)+4b\ \exp(-z_-/w)]+2U_{50}\sigma_5z_-/(z_++z_-). \tag{16}$$

The stress dependence of z_+ and z_- follows from equilibrium conditions $\partial f(\sigma_s)/\partial z_\pm=0$, which leads to two transcendental equations

$$\exp(-z_-/w)=\exp(-z_+/w)+\tilde{\sigma}_5, \tag{17}$$

$$\exp(-z_+/w)(z_+/w+1)+[\exp(-z_+/w)+\tilde{\sigma}_5]\times\{1-\ln[\exp(-z_+/w)+\tilde{\sigma}_5]\}=a(T-T_c)/2, \tag{18}$$

where in analogy to Ref. 8 we have introduced the dimensionless quantity $\tilde{\sigma}_5=(U_{50}w/2b)\sigma_5$. Using the condition $(\partial z_+/\partial\sigma_5)_{z_0}=-(\partial z_-/\partial\sigma_5)_{z_0}$ and Eqs. (15) and (17) we obtain the expression for the elastic compliance S_{55} near the IC-C phase transition:

$$\Delta S_{55}=S_{55}-S_{55}^0=\left(\frac{\partial U_5}{\partial\sigma_5}\right)_{z_0}=N\tilde{S}_{55},\qquad N=(z_++z_-)^{-1}; \tag{19}$$

$$\tilde{S}_{55}=\frac{U_{50}^2w^2}{b}[\exp(-z_-/w)+\exp(-z_+/w)]^{-1},$$

where N is the number of periods per unit length of the crystal and $\tilde{S}_{55}$ is the compliance for the period of $2z_0=z_++z_-$. Opposite temperature dependences of $N(T)$ and $\tilde{S}_{55}(T)$ near T_c explain a maximum in the temperature behavior of S_{55}. For the extremely low values of static stress ($\sigma_{5s}\to 0$) the condition $z_-=z_+=z_0$ takes place and $\exp(z_0/w)=4(z_0/w+1)/a(T-T_c)$. In this case the elastic compliance S_{55} diverges at T_c according to a Curie-Weiss law:

$$\Delta S_{55}=\frac{U_{50}^2w^2}{b}\frac{(z_0/w+1)}{z_0}\frac{1}{a(T-T_c)}. \tag{20}$$

An analogous conclusion follows also from other theories,[5,6] but only for the case without an applied static stress component σ_{5s}.

C. Influence of static stress on the $S_{55}(T)$ anomaly near T_c

The relative temperature changes of real part of effective complex elastic constant $C_r^*(P\|c,q\|a)$, obtained by the TPB method, are shown in Fig. 11 for different values of static load P_s. The experimental geometry corresponds to the component of static stress σ_{5s}, which is proportional to P_s. From experimental data it follows that near T_c the anomalous changes in the real part of the above-mentioned effective elastic constant gradually decrease with increasing of static load, while the thermal hysteresis (ΔT_c) does not change. Those peculiarities persist also for the temperature dependences of the relative elastic compliance S_{55}^r (Fig. 12) calculated from experimental data (Fig. 11). The maximum of S_{55}^r decreases and shifts to the high-temperature region under applied static load. This results can be easily understood in the framework of the soliton theory, presented above. Under an applied static stress σ_{5s}, z_+ becomes infinite at T_c (σ_{5s}), while z_- remains finite as follows from Eq. (17). Consequently $\tilde{S}_{55}$ [see Eq. (19)] is finite at $T=T_c(\sigma_{5s})$ [$\tilde{S}_{55}(T_c)=2U_{50}w/\sigma_{5s}$], and since N decreases with decreasing of temperature ($N\to 0$ if $T\to T_c$), the elastic compliance S_{55} reaches a maximum and then goes to a background value S_{55}^0. The maximum value of S_{55} decreases with increasing $\sigma_{5s}(\Delta S_{55}\sim 1/\sigma_{5s})$ and shifts to higher temperatures

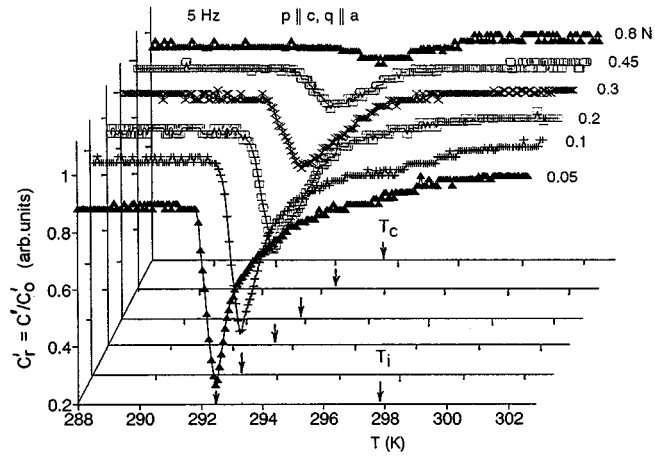

FIG. 11. Temperature dependences of the real part C_r' of the relative complex effective elastic constant $C_r^*(P\|c,q\|a)$ (on heating) measured for different static load ($P_s\|c$) in the TPB method. C_0' corresponds to $T=302$ K. Sample dimensions: $L=5$ mm, $b=1.75$ mm, $h=0.78$ mm.

[$T_c(\sigma_{5s})=T_c(0)+(U_{50}w\sigma_{5s}/ab)\ln(2b/wU_{50}\sigma_{5s})$ (see Ref. 8)] in good qualitative agreement with experimental results above. Thus we may conclude that the real behavior of $S_{55}(T)$ near T_c in the presence of a static stress σ_{5s} corresponds to the case of "clamped" compliance. In other words the obtained results confirm the point of view that domain walls near T_c do not move over macroscopic distances. In addition none of the walls escape or is created inside the crystal. They can oscillate only around their equilibrium positions corresponding to σ_{5s}. In this sense the anomalous behavior of the shear elastic compliance S_{55} near the IC im-

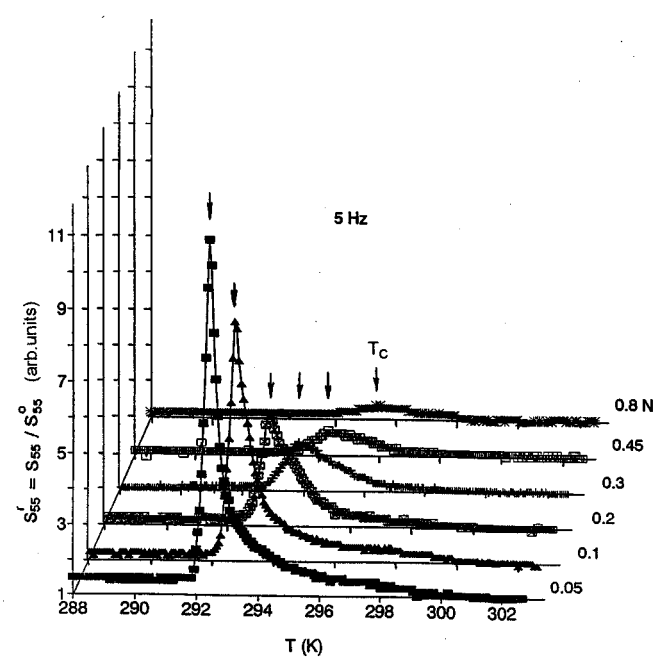

FIG. 12. Temperature dependences of the relative elastic compliance S_{55} (on heating) calculated from experimental data (Fig. 11) for different static load applied along the c axis in the TPB method.

proper ferroelastic phase transition under applied static stress σ_{5s} is quite similar to the behavior of the dielectric susceptibility in the region of IC improper ferroelectric phase transition in a biasing electric field E_s applied parallel to spontaneous polarization.[7] It must be noted, that both elastic and dielectric properties in corresponding cases for $\sigma_{5s} \neq 0$ and $E_s \neq 0$ cannot be explained by other soliton-type theories proposed earlier, e.g., by Hudak[5] and Prelovsek.[6]

IV. CONCLUSION

Using the PPS and TPB methods we have studied the low-frequency elastic properties of the IC ferroelastic crystal TMATC-Cu in the region of the successive phase transitions into the IC phase. Similarly to elastic properties at ultrasonic frequencies (10 MHz), the elastic anomalies at low frequencies (5 Hz) near the P-IC phase transition (at T_i) are well explained within the framework of plane-wave approximation considering the interaction between strain component and soft mode (amplitudon). On the other hand the low-frequency elastic properties in the region of IC-C improper ferroelastic transition (at T_c) can only be explained in terms of a soliton theory. The present work gives a complete picture concerning the temperature behavior of the shear elastic compliance S_{55} around both IC phase transitions. We have revealed that the anomalous behavior of the elastic compliance S_{55} near the IC-C improper ferroelastic phase transition has the same peculiarities as the dielectric susceptibility behavior in the region of IC-C improper ferroelectric phase transition. This similarity, particularly includes the same special form of elastic and dielectric anomalies near T_c at cooling and heating runs, global thermal hysteresis phenomena around the IC-C phase transition and the Curie-Weiss-type behavior of elastic compliance (for IC improper ferroelastics) and dielectric susceptibility (for IC improper ferroelectrics) above T_c. Under applied biasing shear stress σ_{5s} the anomaly $S_{55}(T)$ near the IC-C transition gradually decreases and shifts to higher temperatures like the dielectric constant in IC ferroelectrics under an applied biasing electric field.[7] The last results find their explanation in the framework of soliton theory proposed by Holakovsky and Dvorak[8] initially for the IC improper ferroelectrics and transformed in our work to the case of IC improper ferroelastics. The obtained results confirm the conclusion that the behavior of $S_{55}(T)$ near T_c in applied static stress σ_{5s} corresponds to the case of a ''clamped'' elastic compliance. This implies that the discommensurations (domain walls) can oscillate only around their equilibrium positions corresponding to σ_{5s}, while the total number of discommensurations is not changed in the presence of an oscillating stress $\delta\sigma_5$.

However, there are still some open questions. Particularly, the origin of the anomaly observed near T_c in the imaginary part of the complex effective elastic constant $C_r^*(P\|c,q\|a)$ is unclear. The latter is independent of frequency which cannot be explained by frequently used relaxation-type mechanisms with a single relaxation time. The solution of this problem would probably be found by a theoretical consideration in the framework of a soliton model or a model with coexisting phases.

ACKNOWLEDGMENTS

The authors are indebted to the Osterreichisches Bundesministerium fur Wissenschaft und Forschung for support. The present work was supported by the Osterreichischen Fonds zur Forderung der Wissenschaftlichen Forschung under Project No. P8285-TEC. Two authors (A.V.K. and V.P.S.) would like to express their gratitude to colleagues at the Institute fur Experimentalphysik, Universitat Wien, for kind hospitality during their stay at this Institute. Useful discussions with Professor R. Blinc are also greatly appreciated.

*Permanent address: Institute of Physical Optics, Dragomanova str. 23, 290005, Lviv, Ukraine.

[1] W. L. McMillan, Phys. Rev. B **14**, 1496 (1976).
[2] A. D. Bruce, R. A. Cowley, and A. F. Murray, J. Phys. C **11**, 3591 (1978).
[3] A. Levstic, P. Prelovsek, C. Filipic, and B. Zeks, Phys. Rev. B **25**, 3416 (1982).
[4] K. Hamano, Y. Ikeda, T. Fujimoto, K. Ema, and S. Hirotsu, J. Phys. Soc. Jpn. Suppl. B **49**, 10 (1980).
[5] O. Hudak, J. Phys. C **16**, 2641 (1983).
[6] P. Prelovsek, J. Phys. C **16**, 3257 (1983).
[7] J. Fousek and J. Kroupa, J. Phys. C **21**, 5450 (1988).
[8] J. Holakovsky and V. Dvorak, J. Phys. C **21**, 5449 (1988).
[9] K. Gesi and M. Iizumi, J. Phys. Soc. Jpn. **48**, 1775 (1980).
[10] W. Rehwald and A. Vonlanthen, Z. Phys. B Condens. Matter **61**, 25 (1985).
[11] A. Gomez-Cuevas, M. J. Tello, J. Fernandez, A. Lopez-Echarri, J. Herreros, and M. Couzi, J. Phys. C **16**, 473 (1983).
[12] A. Sawada, J. Sugiyama, M. Wada, and Y. Ishibashi, J. Phys. Soc. Jpn. **48**, 1773 (1980).
[13] A. Sawada, J. Sugiyama, M. Wada, and Y. Ishibashi, J. Phys. Soc. Jpn. **49**, Suppl. B, 89 (1980).
[14] J. Sugiyama, M. Wada, A. Sawada, and Y. Ishibashi, J. Phys. Soc. Jpn. **49**, 1405 (1980).
[15] O. G. Vlokh, A. V. Kityk, O. M. Mokry, and V. G. Grybyk, Phys. Status Solidi A **116**, 287 (1989).
[16] O. M. Mokry, Ph.D. thesis, Lviv University, 1991.
[17] E. P. Papadakis, J. Acoust. Soc. Am. **42**, 1405 (1967).
[18] D. W. Wilson and L. A. Carlsson, in *Determination of Elastic and Mechanical Properties*, edited by B. W. Rossiter and R. C. Baetzold, Physics Methods of Chemistry Vol. VII (Wiley, New York, 1991), p. 180.
[19] V. Dvorak and J. Petzelt, J. Phys. C **11**, 3609 (1978).
[20] W. Rehwald, A. Vonlanthen, J. K. Kruger, R. Wallerius, and H. G. Unruh, J. Phys. C **13**, 3823 (1980).
[21] V. V. Lemanov and S. Kh. Esayan, Ferroelectrics **73**, 125 (1987).
[22] A. V. Kityk, V. P. Soprunyuk, and O. G. Vlokh, J. Phys. Condens. Matter **5**, 235 (1993).
[23] S. Kh. Esayan (unpublished).
[24] J. Fousek, J. Kroupa, and J. Chapelle, Solid State Commun. **63**, 769 (1987).
[25] Y. Ishibashi, in *Incommensurate Phases in Dielectrics*, edited by R. Blinc and A. Levanyuk (North-Holland, Amsterdam, 1986), Vol. 2, p. 49.